+ model

ARTICLE IN PRESS

Available online at www.sciencedirect.com

SCIENCE DIRECT®

PALAEO

Palaeogeography, Palaeoclimatology, Palaeoecology xx (2005) xxx–xxx

www.elsevier.com/locate/palaeo

Carbon isotope chemostratigraphy in Arctic Canada: Sea-level forcing of carbonate platform weathering and implications for Hirnantian global correlation

Michael J. Melchin [a,*], Chris Holmden [b]

[a] *Department of Earth Sciences, St. Francis Xavier University, Antigonish, Nova Scotia, Canada, B2G 2W5*
[b] *Saskatchewan Isotope Laboratory, Department of Geological Sciences, University of Saskatchewan, 114 Science Place, Saskatoon, Canada, SK S7N 5E2*

Received 25 October 2004; received in revised form 7 October 2005; accepted 12 October 2005

Abstract

Three sections through latest Ordovician strata in the Canadian Arctic Islands have been studied for carbon isotopes, derived from the organic matter ($\delta^{13}C_{org}$) and whole-rock carbonate ($\delta^{13}C_{carb}$) fractions. The sections are well constrained biostratigraphically using graptolites, lithostratigraphically and palaeogeographically. $\delta^{13}C_{org}$ data appear to provide a signal that mainly reflects chemical changes in the seawater, whereas the $\delta^{13}C_{carb}$ data seem to have been variably affected by sediment reworking and diagenesis. Results show that a positive $\delta^{13}C_{org}$ excursion of 3–6‰ begins just below the base of the Hirnantian Stage and peaks in the lower part of the *Normalograptus extraordinarius* biozone of lower Hirnantian. This is followed by an interval of reduced $\delta^{13}C$ values and a second peak of similar magnitude, which occurs in the lower *Normalograptus persculptus* biozone (upper Hirnantian). These peaks appear to correlate well with episodes of glacial expansion described from West Africa.

Global correlation between $\delta^{13}C$ curves suggests that the timing of peak positive excursions is not completely synchronous between different regions. In particular, the lower Hirnantian peak seen in Arctic Canada and some other areas appears to be suppressed in sedimentary successions from the circum-Iapetus region, where peak values occur in later Hirnantian time. Thus, no single, regional $\delta^{13}C$ curve can reliably serve as a benchmark for high-resolution, global correlation.

These data provide support for the hypothesis that the positive $\delta^{13}C$ shifts seen in these sections and many others worldwide are the result of increased rates of weathering of carbonate platforms that were exposed during the glacio-eustatically controlled sea-level fall. This caused the isotope value of the C-weathering flux to shift towards the ^{13}C-enriched carbonate end-member, increasing the $\delta^{13}C$ value of carbon transported by rivers to both epeiric seas and the oceans. Magnitude differences between Hirnantian $\delta^{13}C$ excursions in shallower and deeper water parts of epeiric sea basins, as well as between different regions, may be explained by water mass differentiation between those regions. The positive shift in the $\delta^{13}C$ value of the Hirnantian oceans is predicted to be about 2–3‰, which is about half the value of the larger excursions found in basin proximal settings of low latitude epeiric seas.

Keywords: Ordovician; Hirnantian; Carbon isotopes; Correlation; Graptolites

1. Introduction

The Late Ordovician was a time of mass extinction, associated with a widespread continental glaciation that

* Corresponding author.
E-mail addresses: mmelchin@stfx.ca (M.J. Melchin), chris.holmden@usask.ca (C. Holmden).

0031-0182/$ - see front matter © 2005 Elsevier B.V. All rights reserved.
doi:10.1016/j.palaeo.2005.10.009

occurred within what was otherwise a prolonged period of greenhouse climatic conditions (Sheehan, 2001). Evidence from sedimentological, faunal, and geochemical data all suggest that the major phases of glaciation occurred within the early to middle part of the Hirnantian Epoch (e.g., Brenchley et al., 1994; Ghienne, 2003). Knowledge of the temporal relationships of the biodiversity and palaeoenvironmental changes and how these correlate globally are central to understanding the processes that drove these changes. Carbon isotope chemostratigraphy has become an important tool in the study of bioevents because it can play a role both in their global correlation and also helps to constrain the possible nature and range of palaeoenvironmental changes. New carbon-isotope chemostratigraphic data from Arctic Canada are presented that are well-constrained by graptolite biostratigraphy. These results, combined with new biostratigraphic data for Dob's Linn, Scotland, and Anticosti Island, Quebec, yield insights into the relative timing of the carbon isotope excursions and graptolite biostratigraphy in those regions, as well as globally. The results cast doubt on the hypothesis that the timing and form of a composite curve based on the Baltic succession can be used as a benchmark for global correlation through the Hirnantian (Brenchley et al., 2003).

2. Materials and methods

Samples for the present study were collected from the lower member of the Cape Phillips Formation during the summer of 1998 from three localities in the central region of the Queen Elizabeth Islands, Nunavut, Canada: two sections from northeastern Cornwallis Island; and one from Truro Island (Fig. 1). The general stratigraphy and palaeogeographic setting of the Cape Phillips Formation in this region were described by Melchin (1989), Melchin et al. (1991), and Coniglio and Melchin (1995). The three study sections occur in

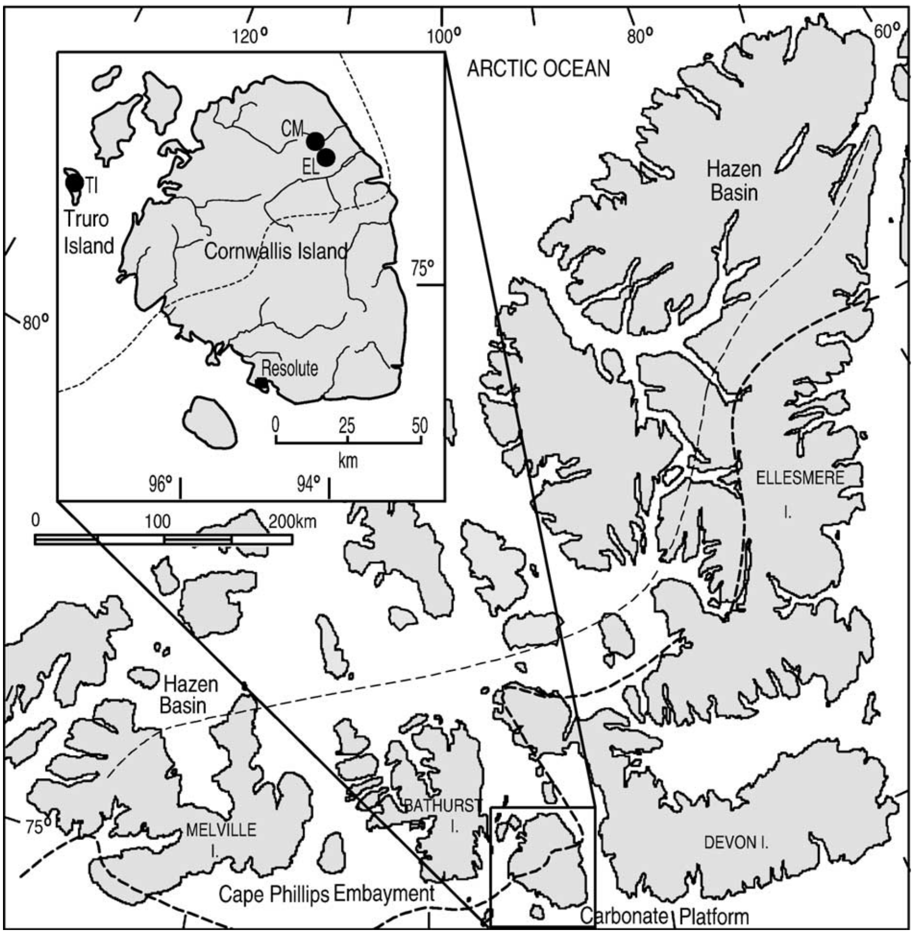

Fig. 1. Map showing locations of study sections on Cornwallis and Truro islands, Nunavut, Arctic Canada, and the general palaeogeography of the Cape Phillips Embayment in relation to the shallow carbonate platform and the deep-water Hazen Basin in Late Ordovician time. EL–Eleanor Lake; CM–Cape Manning; TI–Truro Island. Palaeogeography from Melchin (1989) and De Freitas et al. (1999).

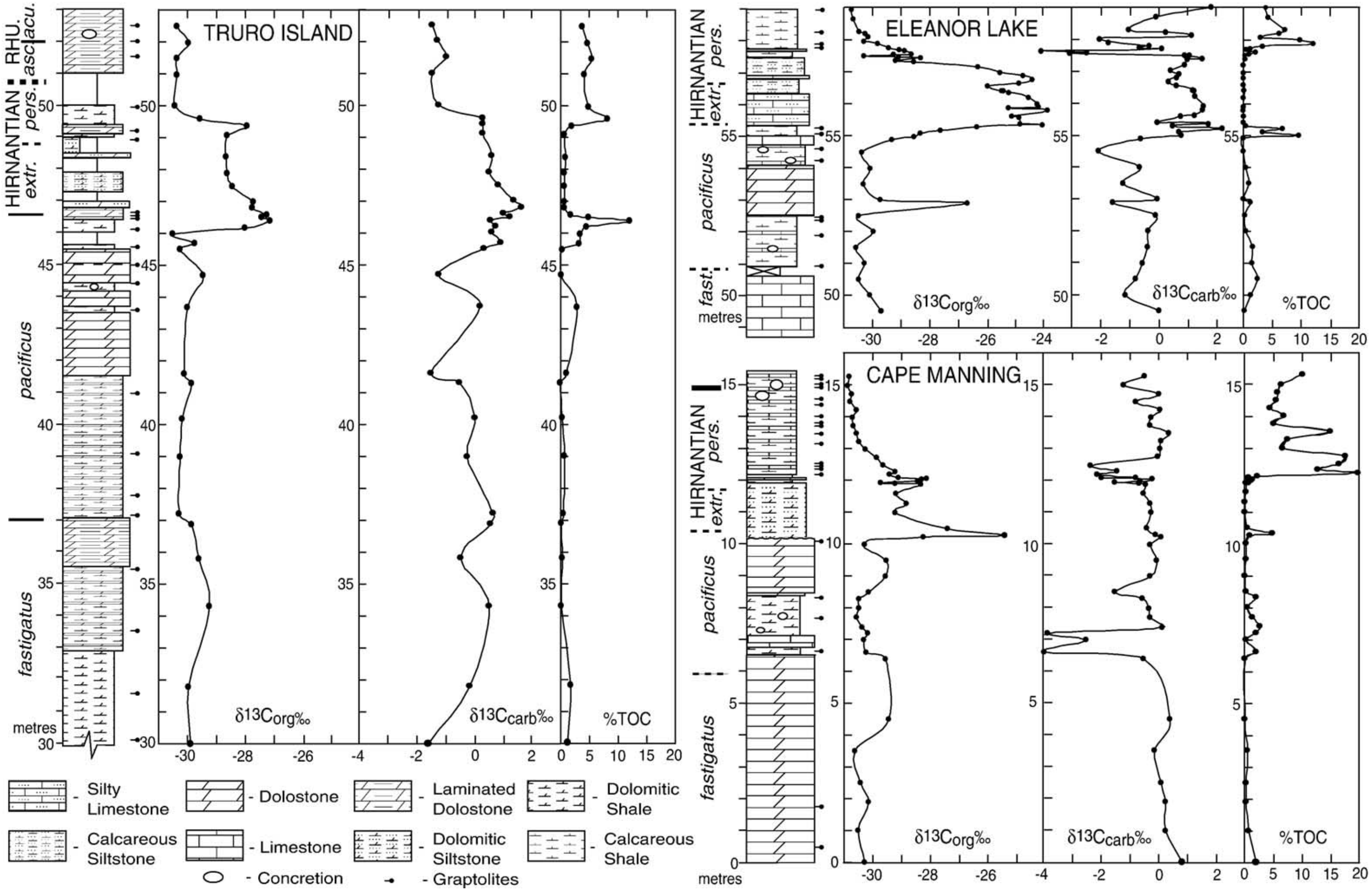

Fig. 2. Graptolite biostratigraphy, lithostratigraphy, carbon isotope chemostratigraphy (from organic matter and whole-rock carbonate), and total organic carbon values from the three study sections, Truro Island, Eleanor Lake, and Cape Manning. The Hirnantian Stage is shown as defined by Cooper and Sadler (2004). The underlying stage has yet to be formally named and is not labelled here. Abbreviations: *extr.–N. extraordinarius* Biozone; *pers.–N. persculptus* Biozone; *asc.–A. ascensus* Biozone; *acu.–P. acuminatus* biozone; Rhu–Rhuddanian Stage, the lowest stage of the Silurian.

the south-central part of the Cape Phillips Embayment, a southern extension of the Early Palaeozoic Franklinian Basin (De Freitas et al., 1999). During the latest Ordovician and Early Silurian, this region represented a distal ramp environment that was intermittently above and below storm wave base as sea level fluctuated. During the episodes of higher sea level, the strata were dominated by laminated, organic-rich, graptolitic, calcareous or dolomitic shales, whereas strata deposited during episodes of lower sea level are either bioturbated, micritic carbonates or, as seen in many of the Hirnantian samples, silty, dolomitic limestones or calcareous siltstones (Fig. 2).

Samples for carbon isotopic analysis from both organic matter and whole-rock carbonate fractions were collected from the mid-Ashgill (upper *Anticostia fastigata* or lower *Paraorthograptus pacificus* biozone) to the *Parakidograptus acuminatus* biozone in the Rhuddanian (Lower Llandovery, Lower Silurian).

To prepare samples for C-isotope analysis, whole-rock samples were powdered in an automated agate and mortar device. For organic C-isotope analysis, approximately 5 g of powder was accurately weighed and digested in HCl to remove carbonate minerals, and the residue was rinsed thoroughly and dried. The weight fraction of the residue was determined by gravimetry, and the residue (containing the organic fraction) was re-powdered to ensure homogeneity. The $\delta^{13}C$ of organic matter was measured after conversion to CO_2 using a combustion furnace (ANCA-GSL) attached to a Europa Scientific 20-20 continuous flow isotope ratio mass spectrometer. The weight percent of TOC in the samples was determined comparing the voltages for the sum of the ion beam intensities of masses 44, 45, and 46 CO_2^+ between the samples and a gravimetric standard with a known wt. % carbon. The TOC uncertainty is $\pm 1.3\%$ (1σ). $\delta^{13}C_{carb}$ analyses were performed with a Finnigan Delta E instrument in dual-inlet mode. Sample CO_2 gas was prepared according to the method of McCrea (1950). Carbon isotope results are reported in the standard delta (δ) notation as per mil deviations relative to V-PDB.

External precision for $\delta^{13}C_{carb}$ is better than $\pm 0.2‰$ based on analysis of NBS-19, which yielded $1.95 \pm 0.12‰$ (2σ), over the course of this work. External precision for $\delta^{13}C_{org}$ is better than $\pm 0.3‰$ (2σ) based on 26 analyses of an internal laboratory standard calibrated against IAEA CH-6.

3. Results

Biostratigraphic data record a succession of five regional graptolite biozones through the study interval (Fig. 2), the *A. fastigata* biozone, *P. pacificus* biozone, the *Normalograptus extraordinarius* biozone, and the *Normalograptus persculptus* biozone, which can be readily correlated with other global zonations. The Hirnantian Stage, as recently proposed by Chen et al. (2004) and employed by Cooper and Sadler (2004), includes strata of the *N. extraordinarius* and *N. persculptus* biozones.

Graptolites indicative of the *N. extraordinarius* biozone, which is early Hirnantian in age, occur only in the Truro Island section, where the biozone is indicated by the co-occurrence of *Normalograptus ojsuensis* and *Normalograptus mirnyensis*. Immediately underlying strata of the same lithology contain *Climacograptus pogrebovi*. This species has been previously reported elsewhere only from the uppermost *P. pacificus* biozone, together with the first occurrence of *N. ojsuensis*, just below the first appearance of *N. mirnyensis* and *N. extraordinarius* (Koren' et al., 1983). Thus, it appears that this section shows continuous deposition across the base of the Hirnantian Stage. Strata assigned to the lower *N. extraordinarius* biozone at Truro Island consist of grey-brown dolomitic mudstones and silty dolostones. Lithostratigraphic and chemostratigraphic correlations (Fig. 3), as well as graptolite data from under- and overlying strata, suggest that this biozone is represented by unfossiliferous, silty limestones at Eleanor Lake on Cornwallis Island.

$\delta^{13}C_{org}$ data show that the mean values for most of the pre-Hirnantian portion of the Late Ordovician from all three sections is $-30‰$, with values normally ranging from $-29.5‰$ to $-30.7‰$, although one sample from the *P. pacificus* biozone has a value of $-26.7‰$. The significance of this single, elevated value is not clear.

At both the Truro Island and Eleanor Lake sections, a significant positive carbon isotope excursion occurs within the interval spanning the black shales of the upper *P. pacificus* biozone and the dolomitic mudstones/silty limestones of the *N. extraordinarius* biozone. At Eleanor Lake, this interval reaches a peak value of $-23.9‰$, a positive shift of approximately 5.5–6.5‰ from pre-Hirnantian levels. At Truro Island, the positive shift from pre-Hirnantian to lower Hirnantian values is approximately +3‰. Overlying these silty limestones at Eleanor Lake is a succession of unfossiliferous, calcareous siltstones. The lowest part of these siltstones shows a negative shift of up to 2.1‰ in carbon isotope values, which appears to be equivalent to a thicker interval of similarly reduced values from dolomitic siltstones at Truro Island. Data from a core drilled 2 km north of the Truro Island section indicate

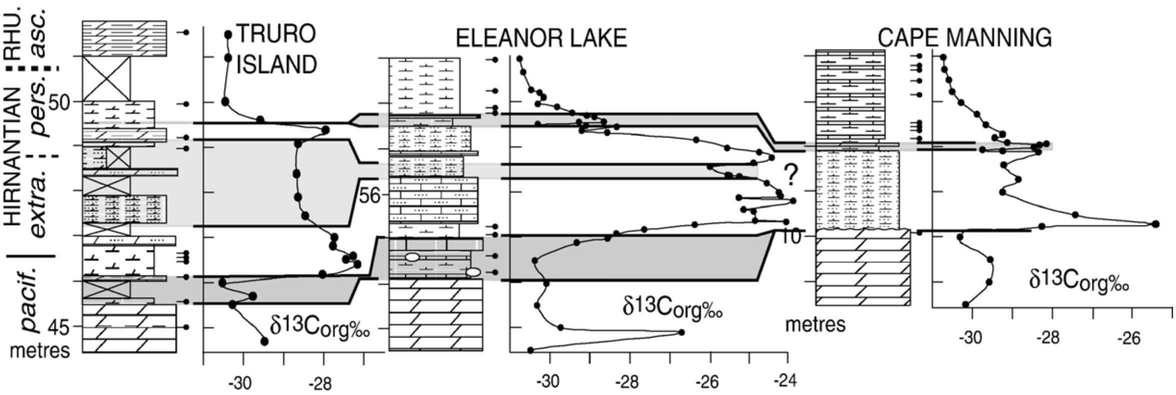

Fig. 3. Proposed correlation of the three study sections through the Hirnantian based on combined biostratigraphic, lithostratigraphic, and chemostratigraphic criteria (see text for discussion). For legend of lithologic symbols and abbreviations, see Fig. 2.

that at least the upper portion of the siltstone unit can be assigned to the lower part of the *N. persculptus* biozone. Unfortunately, this interval could not be sampled at the Truro Island outcrop section due to lack of exposure. At Eleanor Lake, the middle portion of the siltstone returns to more positive C-isotope values, up to −24.4‰, which then decline to pre-Hirnantian levels in the upper part of the unit.

At Cape Manning, the interval of the upper *P. pacificus* biozone that is elsewhere lithologically represented by black shales and the silty limestones of at least part of the *N. extraordinarius* biozone appear to be condensed into a 1–2-cm-thick interval of dissolution surfaces and silty limestone, which are overlain by calcareous siltstones that show a peak of elevated C-isotope values, up to approximately −25‰.

At Truro Island, the siltstone unit is overlain by a dark grey, laminated muddy dolostone unit that demonstrably occurs within the lower part of the *N. persculptus* biozone. This unit shows a positive shift of values up to −27.9‰, which then decline to values generally below the pre-Hirnantian baseline levels.

Overlying the siltstone unit at Eleanor Lake and Cape Manning is a thin, recessive calcareous shale unit overlain by a thin, resistant dolostone unit, followed by black, graptolitic, calcareous or dolomitic shales. Carbon isotope values fluctuate through this interval, with a minor peak occurring within and immediately below the dolostone bed, and then decline gradually in the overlying black shales, which contain graptolites indicative of the *N. persculptus* biozone.

Based on these correlations, it appears that the most complete succession through the Hirnantian C-isotope excursion is represented at Eleanor Lake. At that section, the positive C-isotope excursion that occurs within the Hirnantian interval can be resolved into two prominent peaks. An interval of high-frequency variability of values occurs in the transition into the overlying graptolitic shales of the upper Hirnantian. Graptolite data from Truro Island clearly show that the lower of these peaks begins within the transition from the upper *P. pacificus* biozone into the lower *N. extraordinarius* biozone and the second peak occurs within the *N. persculptus* biozone.

Results of the analyses of $\delta^{13}C_{carb}$ provide less consistent results than the $\delta^{13}C_{org}$ data (Fig. 2). At Eleanor Lake, pre-Hirnantian $\delta^{13}C_{carb}$ values vary between 0‰ and −2‰ and rise sharply in the uppermost *P. pacificus* biozone to a peak of 2.2‰. Above that, values fluctuate between approximately 0.1‰ and 1.5‰ up to the top of the siltstone unit. There is a negative shift in the siltstone unit, as seen in the $\delta^{13}C_{org}$ data, but it seems to occur at a slightly higher level in the $\delta^{13}C_{carb}$ values. In the thin, overlying shale and dolostone beds, the $\delta^{13}C_{carb}$ values dip to a low of −4.0‰ and then fluctuate markedly through the overlying black, graptolitic shales of the *N. persculptus* biozone.

As at Eleanor Lake, the Truro Island $\delta^{13}C_{carb}$ values vary through the pre-Hirnantian strata and become slightly elevated through the dolomitic mudstone/siltstone unit, with a peak in the lower Hirnantian. Unlike Eleanor Lake, there is no strong negative peak above the siltstone unit and values simply return to preexcursion levels.

At Cape Manning there is no positive shift in $\delta^{13}C_{carb}$ values at all in the Hirnantian. A strong negative shift occurs within the lower *P. pacificus* biozone and another weaker one in the beds overlying the siltstone unit, as at Eleanor Lake. Otherwise, values through the whole study interval fluctuate mainly between approximately −0.8‰ and +0.4‰.

4. Regional and global correlation of Hirnantian C-isotope curves

4.1. Regional correlations

Using the combined biostratigraphic, lithological, and carbon isotope data (particularly $\delta^{13}C_{org}$), it is possible to propose a high-resolution correlation of the study sections through the interval from the upper *P. pacificus* biozone into the *N. persculptus* biozone (Fig. 3). This correlation suggests that strata equivalent to the uppermost *P. pacificus* biozone and some or possibly all of the *N. extraordinarius* biozone are missing at Cape Manning and that significant variations in thickness of the other units occur between the sections. Since these units represent relatively shallow-water, subtidal siltstone-carbonate units that were deposited during the early Hirnantian sea-level lowstand, it is not surprising that local hiatuses and thickness variations should result from shifting of offshore sediment bodies and shelf current systems.

The overall pattern represented by the $\delta^{13}C_{org}$ data suggests a positive shift through the interval spanning the base of the Hirnantian, beginning in the uppermost *P. pacificus* biozone and peaking in the lower *N. extraordinarius* biozone. The magnitude of this positive shift is approximately 6‰ above pre-Hirnantian baseline values at Eleanor Lake, but only approximately +3‰ at Truro Island, a deeper water section. As noted above, the biostratigraphic and lithostratigraphic evidence suggests that the sedimentation and sampling are continuous through the lower Hirnantian at Truro Island, so the lower magnitude of the excursion at that section does not appear to be the result of a gap in the record at that section.

Following a negative shift of approximately 2.1‰ a second positive excursion to a value of −24.4‰ is seen in somewhat higher Hirnantian strata at Eleanor Lake, which is thought to be correlative with the second peak observed at Truro Island (Fig. 3).

It is not clear from the evidence available whether the single strong peak in $\delta^{13}C_{org}$ values seen at Cape Manning is correlative with the lower peak at Eleanor Lake or with the upper one. The fact that the Cape Manning peak occurs in siltstone rather than silty limestones suggest that it may be correlative with the upper peak at Cape Manning, which would imply that all of the strata equivalent to the *N. extraordinarius* biozone are missing at a disconformity at the base of the siltstone. On the other hand, the presence of what appears to be a significant trough in $\delta^{13}C_{org}$ values above the peak at Cape Manning suggests that it may be the upper peak which is missing, possibly at a cryptic paraconformity at the top of the siltstone unit.

An interval of high-frequency variability is seen in the lower *N. persculptus* biozone at Eleanor Lake and Cape Manning, but could not be recognized at Truro Island due to the lower resolution of sampling at the latter section.

4.2. Global correlations

Both $\delta^{13}C_{carb}$ and $\delta^{13}C_{org}$ data have been previously published from a number of sections around the world, including Estonia and Latvia (Brenchley et al., 2003), Scotland (Underwood et al., 1997), Anticosti Island, Canada (Long, 1993a), Nevada, USA (Finney et al., 1999), and South China (Wang et al., 1997). Brenchley et al. (2003) proposed that among the known sections from which C-isotope data had been obtained, the most complete succession is located in Estonia, where the excursion spans the *N. extraordinarius* and lower *N. persculptus* biozones. It was further suggested that the Estonian succession could be used as a benchmark for high-resolution global correlation as well as a means by which the completeness of other sections could be measured. Although the Estonian and Latvian sections are well constrained by chitinozoan biostratigraphy, their correlation with the graptolite biozonation can only be achieved indirectly, making it difficult to test the proposed correlations of Brenchley et al.

Melchin et al. (2003) briefly presented a revised global correlation of graptolite and chitinozoan biozonations and C-isotope curves, based on new biostratigraphic data from Scotland, Anticosti Island, Canada, and Arctic Canada, as well as the new carbon isotope data reported in this paper. On Anticosti Island some of the graptolites previously assigned to *Normalograptus angustus* in the upper ca. 15 m the Ellis Bay Formation (Riva, 1988) have been reidentified by Zalasiewicz and Tunnicliff (1994) as *Normalograptus parvulus*. In addition, Melchin (2002) identified *Normalograptus minor* approximately 15 m below the top of the Ellis Bay Formation. Both species have been previously reported from strata not lower than the *N. persculptus* biozone, which suggests that the most significant positive $\delta^{13}C_{carb}$ excursion (whole-rock data—Long, 1993a) in the Anticosti succession is within the *N. persculptus* biozone (Fig. 4). Two weaker positive shifts are also seen in the lower part of the Ellis Bay Formation (in the basal Vellida and upper Prinsta members–Long, 1993a,b, figs. 10,11), which, based on brachiopod data, are lower Hirnantian (*N. extraordinarius* biozone) (Copper, 2001; Jin and Copper, 2004). These

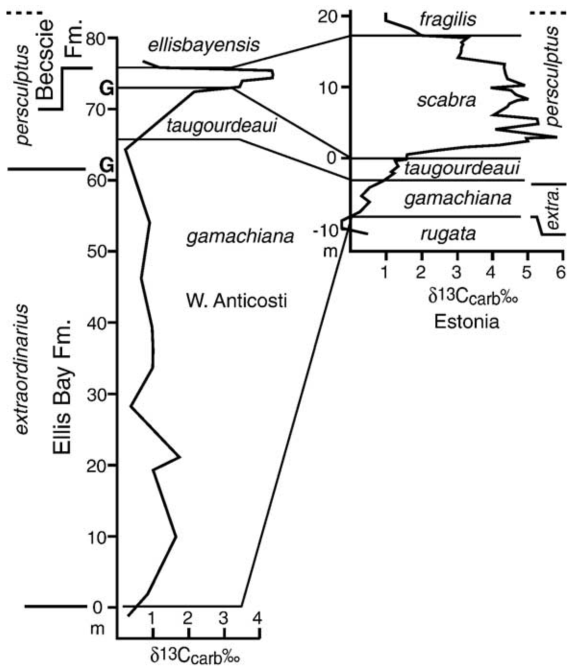

Fig. 4. Proposed correlation of Hirnantian strata of western Anticosti Island, Canada, and Estonia, based on combined biostratigraphic and chemostratigraphic criteria. Carbon isotope curve for Anticosti Island from Long (1993a). The Estonia curve is a composite from Brenchley et al. (2003). The data for the interval from the *rugata* to lower *taugourdeaui* biozones are mainly from Kaugatama, Estonia, and the upper *taugourdeaui* to *fragilis* biozones from Ruhnu. Meterages from an aribitrarily chosen datum, top of *taugourdeaui* biozone. Chitinozoan biozones are indicated in horizontal lettering, graptolite biozones in vertical lettering. Note that the *gamachiana* and *taugourdeaui* biozones can be recognized on both Anticosti Island (Soufiane and Achab, 2000) and in Latvia–Estonia (Nõlvak, 1999), whereas the *ellisbayensis* biozone is not recognizable in Lativia–Estonia and the *scabra–fragilis* biozones are not recognizable on Anticosti Island. The correlation between the chitinozoan and graptolite biozones is inferred from combined graptolite and brachiopod data from Anticosti Island (Copper, 2001; Melchin, 2002; Jin and Copper, 2004). G–levels of graptolites indicating *persculptus* biozone.

data further suggest that on Anticosti Island most of the *Belonechitina gamachiana* chitinozoan biozone (Soufiane and Achab, 2000) is lower Hirnantian (in the *N. extraordinarius* biozone) and the uppermost *B. gamachiana* and *Spinachitina taugourdeaui* chitinozoan biozones are upper Hirnantian (in the *N. persculptus* biozone) (Fig. 4). If these graptolite data are correct and the chitinozoan biozones are correlative between Anticosti Island (Soufiane and Achab, 2000) and Baltica (Nõlvak, 1999), then the entire Porkuni Stage, the peak of the main positive C-isotope excursion and much the interval of rising C-isotope values observed in Estonia and Latvia (Brenchley et al., 2003) are also within the *N. persculptus* biozone (Fig. 4). This correlation suggests that the lower Hirnantian interval in the Baltic sections described by Brenchley et al. (2003) is highly condensed. Several of their described sections show discontinuity surfaces within or near the interval of the *B. gamachiana* biozone.

At Dob's Linn, Scotland, which is the Global Stratotype Section for the base of the Silurian System, a published $\delta^{13}C_{org}$ curve shows rising values within the upper *Dicellograptus anceps* biozone (upper *P. pacificus* biozone of this study) and lower *N. extraordinarius* biozone, with a peak in the upper part of that zone, and declining values through the *P. persculptus* biozone (Underwood et al., 1997). However, it has recently been discovered that *N. persculptus* occurs in what has previously been named the "*extraordinarius* band" (Williams, 1983; Melchin et al., 2003), 1.2 m below the base of the Birkhill shale. Therefore, the base of the *N. persculptus* biozone at that section, as defined by the first appearance of *N. persculptus*, appears to occur at or below the base of the "*extraordinarius* band". In addition, *N. extraordinarius* occurs in the uppermost graptolitic strata of what had previously been regarded as the underlying *D. anceps* biozone (Williams, 1983), which should be regarded as the lower *N. extraordinarius* biozone, the recently proposed base of the Hirnantian Substage (Chen et al., 2004). Thus, the peak of the positive carbon isotope excursion at Dob's Linn, which occurs at and immediately below the base of the Birkhill Shale (Underwood et al., 1997, Fig. 2), is entirely within the *N. persculptus* biozone, as defined here, although C-isotope values begin to rise and show smaller peaks within the *D. anceps* and *N. extraordinarius* biozones (Fig. 5).

In contrast to the C-isotope records from Scotland, Baltica, and Anticosti island, but similar to the pattern seen in Arctic Canada, data from South China show two intervals of elevated $\delta^{13}C_{org}$ values, one near the base of the *N. extraordinarius* biozone, and the other higher, near the base of the *N. persculptus* biozone (Wang et al., 1997) (Fig. 5). Note that Chen et al. (2005) have shown by graphic correlation that the upper part of the *Hirnantia–Kinnella* Beds of Wang et al. (1997) are correlative with the lower part of the *N. persculptus* biozone.

At Vinini Creek, Nevada (Finney et al., 1999), it appears that at least one phase of a major, positive $\delta^{13}C_{carb}$ (whole-rock) excursion begins within the *N. extraordinarius* biozone but the peak values occur in the uppermost part of that biozone and the lower part of the *N. persculptus* biozone (Fig. 5). Note that we have chosen to use the deep-water Vinini Creek section (Finney et al., 1999, Fig. 2) as a basis for comparison

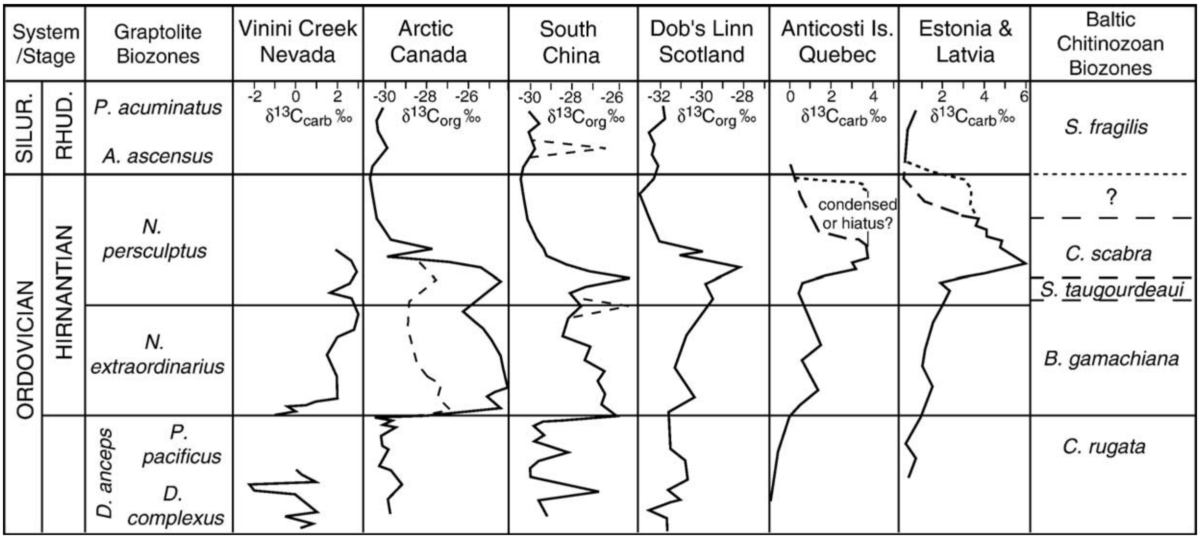

Fig. 5. Proposed correlation of the carbon isotope curves with the graptolite and Baltic chitinozoan biozonation (after Melchin et al., 2003). Sources of carbon isotope data: Vinini Creek, Nevada–Finney et al. (1999); Arctic Canada–this study, mainly based on data from Eleanor Lake (thin dashed line indicates the reduced values seen at Truro Island); South China–Wang et al. (1997), composite data from two sections (dashed lines indicate peaks seen at only one of the two sections); Dob's Linn, Scotland–Underwood et al. (1997); Anticosti Island–Long (1993a), composite of data from two sections (dashed line indicate correlation supported by available biostratigraphic data, dotted line indicates correlation with a significant hiatus as proposed by Brenchley et al., 2003); Estonia and Latvia–Brenchley et al. (2003) (dashed line indicates correlation based on synchroneity of C-isotope profiles, dotted line is based on chitinozoan correlation assuming that the base of *S. fragilis* biozone coincides with the base of the Silurian, as proposed by Brenchley et al., 2003). Abbreviations: Rawth.–Rawtheyan Stage; Rhud.–Rhuddanian Stage; Silur.–Silurian System.

in this study rather than the Monitor Range section (Finney et al., 1999, Fig. 3). Although the latter section shows a more complete succession of C-isotope values, the timing of the excursion relative to both the base of the *N. extraordinarius* biozone and the *N. persculptus* biozone are better constrained at Vinini Creek. Data from the Monitor Range section do suggest, however, that the end of the excursion occurs below the top of the *N. persculptus* biozone, which is not evident from the Vinini Creek data.

At those sections that show apparently continuous deposition of graptolitic strata across the Ordovician–Silurian boundary (e.g., Dob's Linn, Arctic Canada) the C-isotope values decline gradually through the upper part of the *N. persculptus* biozone and reach a low point at or just below the base of the Rhuddanian. On the other hand, at Anticosti Island, the end of the positive C-isotope excursion has been reported to coincide with the Ordovician–Silurian boundary (e.g., Brenchley et al., 2003) (Fig. 5). However, the chitinozoan species *Ancyrochitina ellisbayensis*, which occurs in the strata above the positive δ^{13}C excursion interval on Anticosti Island (Soufiane and Achab, 2000) (Fig. 4), has recently been discovered in the upper part of the *N. persculptus* biozone and lowermost Silurian at Dob's Linn (Verniers et al., 2005), which may suggest that the Ordovician–Silurian boundary occurs in strata several meters above the positive δ^{13}C excursion interval on Anticosti Island, within the range of occurrence of *A. ellisbayensis* (Figs. 4 and 5).

In Estonia and Latvia, the interval of declining δ^{13}C values occurs mainly within the *S. fragilis* chitinozoan biozone, which is generally regarded as lower Silurian (Brenchley et al., 2003). However, if the decline interval in Baltica is coincident with that seen in the graptolitic sections (Fig. 5), then the base of the *S. fragilis* biozone must be within the upper part of the Hirnantian.

5. Discussion

5.1. Impact of detrital carbonate flux and diagenesis on the $\delta^{13}C_{carb}$ excursion

The generally weaker and less consistent positive shifts in the $\delta^{13}C_{carb}$ data, as compared with the $\delta^{13}C_{org}$ values, through the Hirnantian, and the generally more variable values throughout the study section may be accounted for by the fact that these analyses represent whole-rock carbonate data. Sedimentological observations and previous diagenetic studies (Coniglio and Melchin, 1995) suggest that the fine-grained calcite in these sediments derives from at least three sources: primary depositional lime mud, silt-sized grains of detrital calcite and dolomite, and fine-grained carbonate precipitated during shallow burial diagenesis. In addition, many of the carbonate units at the study sections have undergone dolomite replacement of primary calcite. The fact that the lower Hirnantian δ^{13}C excursion in the carbonate fraction is suppressed and less variable relative to that seen in the organic matter may result from the dilution of primary carbonate mud with detrital carbonate, reworked either from within the basin or eroded from the adjacent carbonate platform, which was likely exposed during the early Hirnantian glacioeustatic fall. If this reworked carbonate was deposited prior to the early Hirnantian, then it should show typical pre-Hirnantian C-isotope values.

The strong negative excursions seen in the $\delta^{13}C_{carb}$ data both below and above the lower Hirnantian interval either occur in sediments with elevated organic matter concentrations (Fig. 2) or dolostones. Coniglio and Melchin (1995) showed that bacterial sulphate reduction of organic matter was an important source of early diagenetic, fine-grained calcite in concretions within the same units under study here. In the calcite concretions those units show $\delta^{13}C_{carb}$ values as low as −5.5‰, and so the strongly negative values seen in organic-rich calcareous shales may also be the result of carbon in calcite derived from bacterial decomposition of organic matter under sulphate reducing conditions. The thin dolostone unit that occurs above the siltstone unit at Eleanor Lake and Cape Manning also shows strongly negative $\delta^{13}C_{carb}$ values. Coniglio and Melchin (1995) showed that replacive dolomites in the Lower Cape Phillips Formation show a wide range of values, mainly between 1 and −3‰, although one as low as −6.4‰ occurred in a replaced dolomite concretion.

5.2. Carbonate weathering and local C-cycling

There are presently three main hypotheses under debate to explain the Hirnantian positive δ^{13}C excursions. Brenchley et al. (1995, 2003) and some other authors proposed that they were caused by increased primary productivity in the surface ocean waters and increased organic carbon storage in the sediments and/or deep ocean waters. Kump et al. (1999) showed quantitatively that an increase of 50–75% in the burial rate of organic carbon is required to explain the 6‰ positive shift in the δ^{13}C value of the ocean. However, as noted by Melchin and Mitchell (1991), Hallam and Wignall (1997), and Munnecke et al. (2003), sediments comprising the Hirnantian glacial interval are characterized globally by lower concentrations of organic matter compared to overlying and underlying strata, and this is also generally true for the Canadian Arctic sections (Fig. 2), especially Eleanor Lake, where the succession is most complete. This is more consistent with decreased, as opposed to increased, rates of organic carbon burial, thus challenging the validity of the productivity/organic-carbon-burial hypothesis. It has been suggested that increased productivity during the Hirnantian resulted in the sequestering of organic matter in the deep ocean, in areas not preserved or yet discovered in the stratigraphic record (e.g., Brenchley et al., 2003). However, unless such organic-rich deposits are discovered or some other independent means of estimating changes in global productivity can be developed, this hypothesis cannot be tested.

Alternatively, Kump et al. (1999) proposed a “weathering hypothesis” to explain both the carbon isotope excursions and the cause of the glaciation event in the Hirnantian. They proposed that high rates of mountain building in the Late Ordovician resulted in increased rates of weathering of silicate rocks, thus increasing rates of consumption of atmospheric CO_2. The resulting reduction of p_{CO_2} triggered the glaciation event, which in turn caused eustatic fall. The falling sea level exposed vast areas of carbonate platform on several palaeocontinents, and the weathering of these carbonate sediments caused the positive C-isotope excursion. Although some authors have debated the question of whether or not these changes in weathering processes could have triggered the glaciation event (e.g., Brenchley et al., 2003), it is the origin of the positive δ^{13}C excursions that is the focus of further discussion below.

A sea-level-driven shift of 6‰ in the δ^{13}C value of the C-weathering flux to the oceans would cause a 6‰ shift in the ocean δ^{13}C value, if all other C-fluxes to the oceans remained equal over the interval of the sea-level regression. The problem with this explanation is that such a large shift in δ^{13}C of the C-weathering flux requires a dramatic increase in the weathering of carbonate sediments on the continents. In most models of ocean C-cycling the δ^{13}C value of the land-derived C-weathering input to the oceans is typically set between −5‰ and −7‰ (Kump and Arthur, 1999), which reflects about 75% weathering of carbonate sediment and limestone bedrock (0‰) and 25% weathering of sedimentary organic matter (−21‰ to −29‰). A 6‰ increase in the δ^{13}C of the C-weathering flux requires that the fractional contribution of carbonate weathering increased from 75% to 96% of the total weathered carbon input to the oceans (Kump et al., 1999). Such a dramatic increase in the weathering of sedimentary carbonates seems too high for the globally averaged C-weathering flux, but there are two ways to decrease the apparent carbonate weathering contribution.

The first was proposed by Kump et al. (1999) who suggested that as silicate bedrock became overrun by ice sheets during the Hirnantian glacial advance, p_{CO_2} would have risen and the isotopic discrimination that accompanies photosynthesis in phytoplankton in the oceans would have increased, thus, lowering the $\delta^{13}C$ value of produced organic matter. This change would have allowed preferentially more ^{12}C to be sequestered into organic matter from the ocean DIC pool, leaving seawater relatively higher in $\delta^{13}C$ value at the same level of primary production in the oceans. The magnitude of the inferred change in the photosynthetic fractionation factor was based on an interpretation of an unusually flat, or unchanging, $\delta^{13}C_{org}$ profile, in relation to a large positive shift in $\delta^{13}C_{carb}$ in a Hirnantian section in Nevada (see Fig. 1 in Kump et al., 1999). The flat $\delta^{13}C_{org}$ profile contrasts markedly, however, with our Canadian Arctic $\delta^{13}C_{org}$ profiles, and those from China (Wang et al., 1997) and Scotland (Underwood et al., 1997), which show large positive isotope excursions similar to the large $\delta^{13}C_{carb}$ excursion in Nevada. It would appear, therefore, that the Nevada $\delta^{13}C_{org}$ profile is anomalous, and perhaps only locally significant, and as such the idea that the photosynthetic fractionation factor changed globally across the Hirnantian interval is not supported by the available data.

Alternatively, we consider it more likely that the large magnitudes of the Hirnantian $\delta^{13}C$ excursions recorded in epeiric sea carbonates do not reflect the size of the $\delta^{13}C$ shift in the contemporaneous oceans. The $\delta^{13}C_{DIC}$ of seawater in epeiric seas may have been subjected to strong overprinting by local C-cycling, and therefore, the oceanic $\delta^{13}C$ value is not always preserved in epeiric sea deposits where most of the Hirnantian $\delta^{13}C$ records are found (Holmden et al., 1998; Panchuk et al., in press-a,b). Furthermore, epeiric sea basins contained smaller water volumes and DIC inventories than the ocean basins. This means that relatively small shifts in $\delta^{13}C$ values of local C-weathering fluxes could drive relatively large shifts in $\delta^{13}C_{DIC}$ values of epeiric seas, if seawater C-exchanges between epeiric seas and oceans were restricted. Studies have shown that in both modern (Patterson and Walter, 1994) and ancient epicontinental settings (Holmden et al., 1998; Immenhauser et al., 2002, 2003; Panchuk et al., in press-a,b) locally acting C-cycles may overprint the ocean carbon signature.

Evidence for locally acting C-cycles in Hirnantian epeiric seas is the variability in magnitudes of $\delta^{13}C$ excursions recorded in different settings (e.g., Wang et al., 1997; Finney et al., 1999; Brenchley et al., 2003; this study). In the Cape Phillips basin, we have measured 3‰ offsets in peak $\delta^{13}C_{org}$ values between the basin-proximal Eleanor Lake section and the more basin-distal Truro Island section. These regional differences between stratigraphically equivalent study sections may reflect different impacts of the C-weathering flux on isotope carbon balances across the epeiric sea. For example, C-cycling in epeiric sea settings near paleoshorelines should have been more greatly influenced by changes in local C-weathering fluxes than coeval settings near continental margins where better circulation with open ocean waters should have damped local C-weathering flux signals. By contrast, there appears to have been no gradient in seawater $\delta^{13}C$ values across the Cape Phillips basin either before or after the excursion, as the baseline $\delta^{13}C_{org}$ values (pre- and post-excursion) between sections are similar. This would be the case if sea levels before and after the glaciation were similar, and if the same fractions of sedimentary carbonate and sedimentary organic matter became re-exposed to weathering in the Cape Phillips watershed following the Hirnantian glaciation.

Changes in the weathering rates of carbonates during the Hirnantian may have also been accompanied by changes in the nature and sources of organic matter within the strata in our study, which may have influenced the $\delta^{13}C$ values. As noted by Pancost et al. (1999), however, such changes are unlikely to be solely responsible for excursions of the magnitude seen in this study, particularly at Eleanor Lake. Furthermore, the same patterns characterize the Hirnantian $\delta^{13}C$ excursions in Baltica that are based on $\delta^{13}C_{carb}$ profiles in limestones (Kaljo et al., 2004). For example, two shallow-water sections show large positive $\delta^{13}C$ excursions of about 5‰, whereas a stratigraphically equivalent deeper water section records an excursion of about 2.5‰. This is similar to the 3‰ excursion at Truro Island in the Cape Phillips Basin and suggests that the $\delta^{13}C_{DIC}$ value of the Hirnantian ocean shifted by about half the amount that is typically recorded in shallow-water deposits of Hirnantian epeiric seas.

In summary, if sea-level forcing of the C-weathering flux is considered in the context of local C-cycling in epeiric seas, then the carbonate weathering model predicts that peak-magnitude values of the Hirnantian $\delta^{13}C$ excursions should vary, that larger excursions will be found in basin-proximal compared to basin distal sections of carbonate-producing epeiric seas, and that inferred shifts in epeiric sea $\delta^{13}C_{DIC}$ may be larger than in contemporaneous oceans. The fact that true ocean sediments are rarely preserved makes this last point difficult to test. But if the Hirnantian $\delta^{13}C$ excursions are viewed in the context of local C-cycling in epeiric seas, then the problem of the large and seemingly implausible increase in carbonate sediment weathering is no longer required, and it is also no longer necessary to invoke p_{CO_2}-driven changes in the photosynthetic fractionation factor to address this issue.

A third hypothesis, proposed by Jeppsson (1987, 1990) and more recently modified and developed by Bickert et al. (1997) and Munnecke et al. (2003), relates the δ^{13}C value of marine shelf sediments to changing climate states. They noted that during Late Ordovician and Silurian times, there would have been a strong vertical δ^{13}C gradient in the oceans, with more positive values in surface waters due to high rates of primary production and sinking of organic matter into deeper waters. They proposed that during relatively humid time intervals (H-periods), low-latitude shelves should be subject to estuarine circulation patterns and would primarily be zones of upwelling, resulting in transport of deep waters with relatively low δ^{13}C values onto the shelf environments. During more arid times (A-periods), antiestuarine circulation would preferentially develop over low-latitude shelves, resulting in transport of surface waters with relatively high δ^{13}C values onto the shelf environments, and a shift of deeper, more δ^{13}C-depleted waters, into the deep slope and basinal settings. Munnecke et al. (2003) note, in support of their model, that in the Baltic carbonate platform setting the isotopic shifts coincide with faunal and facies shifts that are consistent with the proposed climatic changes.

We prefer the carbonate platform weathering hypothesis framed in the context of local C-cycling in epeiric seas as the most likely mechanism for explaining the Hirnantian δ^{13}C excursions because timing of the event coincides well with the stratigraphic evidence for widespread carbonate platform exposure in many regions through this time interval. Therefore, it is likely that there was a very significant change in the δ^{13}C value of the C-weathering flux from the cratons at this time. In addition, the model of Bickert et al. (1997) and Munnecke et al. (2003) does not predict that there should be positive carbon isotope excursions in the organic matter of the deep basinal sediments beyond the shelf edge, coincident with the positive excursions seen in shelf carbonates. Rather, their model suggests that both the surface waters, where the primary production of organic matter takes place, and the bottom waters of the deep seas remained relatively unchanged in carbon isotope composition during the changes in climate state (see Munnecke et al., 2003, Fig. 7). However, the $\delta^{13}C_{org}$ data from the strata at Dob's Linn, which were deposited in an offshore, deep-water, slope or rise setting beyond the shelf edge (Armstrong and Coe, 1997; Underwood et al., 1997) clearly show a positive excursion, apparently coincident with that seen in the Baltic sections (Fig. 5). The fact that the positive excursion occurs in these deep-water sediments, formed beyond the shelf edge, but with a relatively low magnitude (about 3‰ compared with pre-excursion values), does not appear to be consistent the climate state model, but is a prediction of the weathering hypothesis as outlined above, which predicts low magnitude excursions in deeper, basinal settings relative to those of the more proximal portions of epeiric seas.

5.3. Asynchronous stratigraphic distribution of peak δ^{13}C excursions

If changes in weathering patterns resulting from glacioeustatic regression caused the Hirnantian positive δ^{13}C excursion, then the attainment of peak δ^{13}C values may be offset between sedimentary deposits in different epeiric sea basins because of differences in the interplay between local and global influences on C-cycling. For example, because of large differences in C-reservoir size between epeiric seas and ocean basins, the seawater carbon residence time in epeiric seas was predictably shorter than in the contemporaneous oceans (Panchuk et al., in press-a). As a consequence, the ocean response to a shift in the isotope value of the C-weathering flux will lag behind the adjustment in the δ^{13}C value of epeiric seas, especially epeiric seas with strong locally acting C-cycles and restricted C-exchanges with the surface ocean. In epeiric seas with weak local C-cycles the shift in δ^{13}C value will be more in phase with the lag in the ocean response because of the stronger influence of the ocean C-cycle on the local epeiric sea C-cycle. Differences in sedimentation rate, hiatuses, and diachroneity between stratigraphically equivalent deposits may further complicate timing and correlation of δ^{13}C excursions. Therefore, a prediction of this model is that stratigraphically equivalent δ^{13}C excursions may not be isochronous time planes as is widely assumed.

In the regions around the Iapetus Ocean (e.g., Baltica, eastern Laurentia—Fig. 6) the positive δ^{13}C excursions appear to be suppressed within the lower Hirnantian, and some may also show differences in timing within the upper Hirnantian (Fig. 5). This may result from the fact that the Baltic and Anticosti basins show a history of sedimentation and sea-level change that differs from those represented in Arctic Canada, Nevada, and South China. Facies analyses of successions both in the Baltic region (Dahlqvist and Calner,

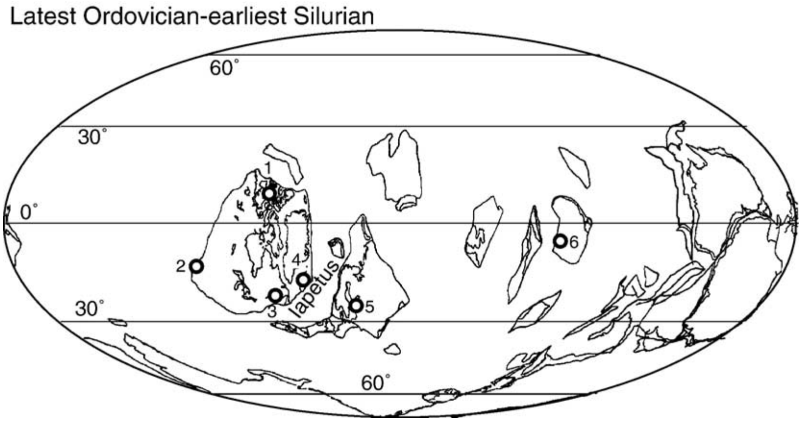

Fig. 6. Global palaeogeographic map for the latest Ordovician–earliest Silurian (from Cocks and Torsvik, 2002) showing locations of the carbon isotope studies referred to in this paper. 1–Canadian Arctic (this study); 2–Vinini Creek, Nevada (Finney et al., 1999); 3–Anticosti Island (Long, 1993a); 4–Dob's Linn, Scotland (Underwood et al., 1997); 5–Estonia and Latvia (Brenchley et al., 2003); 6–Yichang area, South China (Wang et al., 1997).

2004; Kaljo et al., 2004) and Anticosti Island (Long and Copper, 1987; Long, 1993b) show that although there were one or several minor or moderate episodes of sea-level fall within the lower Hirnantian in these regions, the timing of maximum lowstand occurred in later Hirnantian time, coincident with the time of the maximum positive $\delta^{13}C$ excursion (see discussion of correlations above). Those authors attributed the occurrence of relatively high sea levels through the Late Ordovician in these regions to relatively high rates of subsidence, due to crustal loading resulting from nearby Caledonian–Taconic orogenic uplift. This also provided the source for the relatively high proportion of siliciclastic sediments that occur in these basins in much of Late Ordovician time. If the positive $\delta^{13}C$ excursions are primarily the result of an increase in weathering flux of carbonates as a result of widespread exposure of carbonate shelves in early Hirnantian time, it follows that in basins that show high rates of subsidence resulting in reduced carbonate platform exposure combined with high rates of siliclastic input, the positive $\delta^{13}C$ shift should be less pronounced or absent. This may explain why in the circum-Iapetus region through the early Hirnantian, the positive $\delta^{13}C$ excursions are suppressed until later Hirnantian time when sea level was much lower in that area. In addition, differences in water chemistry between the circum-Iapetus basins and other world's oceans may have been maintained as a result of the relatively weak connection between them during Hirnantian time as a result of the progressive closure of the Iapetus and docking of Baltica with Avalonia (Van Staal et al., 1998; Cocks and Torsvik, 2002; Murphy et al., 2004). This restriction may also explain the survival of some endemic, relict benthic faunas through the Hirnantian in eastern Laurentia, Avalonia and Baltica (e.g., Owen and Robertson, 1995).

5.4. Relationship of the $\delta^{13}C$ curve to the record of glaciation

Globally, it appears that the major interval of positive $\delta^{13}C$ excursions and eustatic fall extend from a level near the base of the lower Hirnantian *N. extraordinarius* biozone to a level within the *N. persculptus* biozone (upper Hirnantian), and that $\delta^{13}C$ values decline through the upper Hirnantian strata. Within the $\delta^{13}C_{org}$ values, two prominent peaks can be resolved within the positive excursion interval, which may coincide with pulses of peak glaciation (Fig. 7). Ghienne (2003) described sedimentary successions in West Africa that suggested that there were two major pulses of glacial expansion that caused eustatic fall, one peaking in the early Hirnantian and the second in the mid- to late Hirnantian, and that each was followed by recession (eustatic rise). If the peaks in $\delta^{13}C$ values are the result of increased rates of carbonate platform weathering during glacial maxima and glacioeustatic fall, then the two major events of glacial growth can be recognized within the $\delta^{13}C_{org}$ data from Arctic Canada. This remarkable correspondence provides further support for the sea-level-driven C-weathering hypothesis as the cause of the Hirnantian $\delta^{13}C$ excursions, globally, and it follows, too, that the detailed shape-structure of the Hirnantian $\delta^{13}C$ excursion behaves as a highly sensitive chemostratigraphic sea-level curve. In addition, intervals of high-frequency variability in $\delta^{13}C_{org}$ values occur within the lower peak and above the upper peak at Eleanor Lake. It may be that these correspond

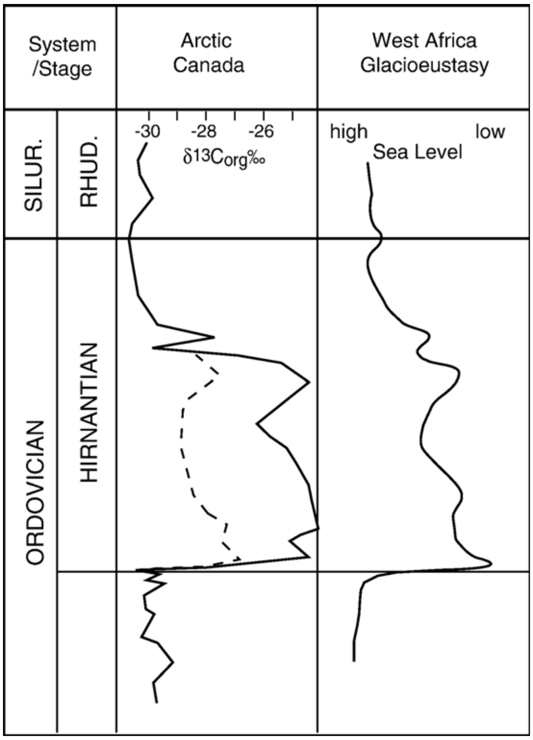

Fig. 7. Proposed correlation of the composite organic carbon isotope curve from Arctic Canada (from Fig. 5) with the glacioeustatic sea level curve proposed by Ghienne (2003)based on analysis of sedimentary successions in the Taoudeni Basin, West Africa.

with lower magnitude events of glacial advance and retreat described by Ghienne (2003) (Fig. 3). Alternatively, these fluctuations may also result from variations in the source material or diagenesis of the organic matter that is associated with the changes in lithology through these intervals.

6. Conclusions

Results of the study of three sections through latest Ordovician strata in the Canadian Arctic Islands show that a positive $\delta^{13}C_{org}$ excursion of 3–6‰ begins just below the base of the Hirnantian Stage and peaks in the lower part of the *N. extraordinarius* biozone of lower Hirnantian. This is followed by an interval of reduced $\delta^{13}C$ values and a second peak of similar magnitude, which occurs in the lower *N. persculptus* biozone (upper Hirnantian).

The peaks in $\delta^{13}C_{org}$ values appear to correlate well with episodes of glacial expansion described from West Africa. These data provide support for the hypothesis that the positive $\delta^{13}C$ shifts seen in these sections and many others worldwide are the result of increased rates of weathering of carbonate platforms that were exposed during the glacio-eustatically controlled sea-level fall. This caused the isotope value of the C-weathering flux to shift towards the ^{13}C-enriched carbonate end-member, increasing the $\delta^{13}C$ value of carbon transported by rivers to both epeiric seas and the oceans. Magnitude differences between Hirnantian $\delta^{13}C$ excursions in shallower and deeper water parts of epeiric sea basins, as well as between different regions, may be explained by water mass differentiation between those regions. The peak magnitude change in $\delta^{13}C$ value of the Hirnantian ocean is predicted to be about 2–3‰, which is about half the value of the larger excursions found in basin proximal settings of low-latitude epeiric seas.

Global correlation between $\delta^{13}C$ curves suggests that the timing of peak positive excursions is not completely synchronous between different regions. In particular, the lower Hirnantian peak seen in Arctic Canada and some other areas appears to be suppressed in sedimentary successions from the circum-Iapetus region, where peak values occur in later Hirnantian time. This may be the result of differences in subsidence and sedimentation histories between the circum-Iapetus basins and other parts of the world, and possibly restriction of ocean circulation into the circum-Iapetus Ocean basins resulting from its gradual closure through Late Ordovician–Early Silurian time. Thus, no single, regional $\delta^{13}C$ curve can reliably serve as a benchmark for high-resolution, global correlation.

Acknowledgements

We thank E.W. MacDonald for his assistance in the field and the Polar Continental Shelf Project for logistical support. We also gratefully acknowledge the Natural Sciences and Engineering Research Council for the financial support to our research programs. C.H. thanks Tim Prokopiuk for his invaluable assistance in the laboratory, and for running some of the analyses. The manuscript has benefited from discussions with P. Copper, comments by M. Saltzman and an anonymous reviewer.

References

Armstrong, H.D., Coe, A.L., 1997. Deep-sea sediments record the geophysiology of the Late Ordovician glaciation. Journal of the Geological Society (London) 154, 929–934.

Bickert, T., Pätzold, J., Samtleben, C., Munnecke, A., 1997. Paleoenvironmental changes in the Silurian, indicated by stable isotopes in brachiopod shells from Gotland (Sweden). Geochimica et Cosmochimica Acta 61, 2717–2730.

Brenchley, P.J., Marshall, J.D., Carden, G.A.F., Robertson, D.B.R., Long, D.G.F., Meidla, T., Hints, L., Anderson, T.F., 1994. Bathymetric and isotopic evidence for a short lived Late Ordovician glaciation in a greenhouse period. Geology 22, 295–298.

Brenchley, P.J., Carden, G.A.F., Marshall, J.D., 1995. Environmental changes associated with the "first strike" of the Late Ordovician mass extinction. Modern Geology 20, 69–82.

Brenchley, P.J., Carden, G.A., Hints, L., Kaljo, D., Marshall, J.D., Martma, T., Meidla, T., Nõlvak, J., 2003. High-resolution stable isotope stratigraphy of Upper Ordovician sequences: constraints on timing of bioevents and environmental changes associated with mass extinction and glaciation. Geological Society of America Bulletin 115, 89–104.

Chen, X., Rong J.-y., Fan J.-x., Zhan R.-b., Mitchell, C.E., Harper, D.A.T., Melchin, M.J., Wang X.-f., 2004. A final report on the GSSP candidate of the Hirnantian Stage. Report to the Subcommission on Ordovician Stratigraphy, http://seis.natsci.csulb.edu/ord2/Documents/Wangjiawan_GSSP.pdf.

Chen, X., Fan, J.-x., Melchin, M.J., Mitchell, C.E., Sheets, H.D., 2005. Patterns and processes of Latest Ordovician graptolite extinction and recovery based on data from South China. Journal of Paleontology 79, 842–861.

Cocks, L.R.M., Torsvik, T.H., 2002. Earth geography from 500 to 400 million years ago: a faunal and palaeomagnetic review. Journal of the Geological Society (London) 159, 631–644.

Coniglio, M., Melchin, M.J., 1995. Petrography and isotope geochemistry of diagenetic carbonates in the lower Cape Phillips Formation, Cornwallis Island, Arctic Archipelago, Canada. Bulletin of Canadian Petroleum Geology 43 (3), 251–266.

Copper, P., 2001. Reefs during the multiple crises towards the Ordovician–Silurian boundary: Anticosti Island, eastern Canada, worldwide. Canadian Journal of Earth Sciences 38, 153–171.

Cooper, R.A., Sadler, P.M., 2004. The Ordovician period. In: Gradstein, F., Ogg, J., Smith, A. (Eds.), A Geologic Time Scale 2004. Cambridge University Press, pp. 165–187.

Dahlqvist, P., Calner, M., 2004. Late Ordovician palaeoceanographic changes as reflected in the Hirnantian–early Llandovery succession of Jämtland, Sweden. Palaeogeography, Palaeoclimatology, Palaeoecology 210, 149–164.

De Freitas, T.A., Trettin, H.P., Dixon, O.A., Mallamo, M., 1999. Silurian system of the Canadian Arctic archipelago. Bulletin of Canadian Petroleum Geology 47 (2), 136–193.

Finney, S.C., Berry, W.B.N., Cooper, J.D., Ripperdan, R.L., Sweet, W.C., Jacobson, S.R., Soufiane, A., Achab, A., Noble, P.J., 1999. Late Ordovician mass extinction: a new perspective from stratigraphic sections in central Nevada. Geology 27, 215–218.

Ghienne, J.-F., 2003. Late Ordovician sedimentary environments, glacial cycles, and post-glacial transgression in the Taoudeni Basin, West Africa. Palaeogeography, Palaeoclimatology, Palaeoecology 189, 117–145.

Hallam, A., Wignall, P.B., 1997. Latest Ordovician extinctions: one disaster after another. In: Hallam, A., Wignall, P.B. (Eds.), Mass Extinctions and their Aftermath. Oxford University Press, pp. 39–61.

Holmden, C., Creaser, R.A., Muehlenbachs, K., Leslie, S.A., Bergström, S.M., 1998. Isotopic evidence for geochemical decoupling between ancient epeiric seas and bordering oceans: implications for secular curves. Geology 26 (6), 567–570.

Immenhauser, A., Kenter, J.A.M., Ganssen, G., Bahamonde, J.R., Vliet, V.A., Saher, M.H., 2002. Origin and significance of isotope shifts in Pennsylvanian carbonates (Austrias NW Spain). Journal of Sedimentary Research 72, 82–94.

Immenhauser, A., Porta, D.G., Kenter, J.A.M., Bahamonde, J.R., 2003. An alternative model for positive shifts in shallow-marine carbonate $\delta^{13}C$ and $\delta^{18}O$. Sedimentology 50, 1–7.

Jeppsson, L., 1987. Lithological and conodont distributional evidence for episodes of anomalous oceanic conditions during the Silurian. In: Aldridge, R.J. (Ed.), Palaeobiology of Conodonts. Ellis Horwood Ltd., Chichester, pp. 129–145.

Jeppsson, L., 1990. An oceanic model for lithological and faunal changes tested on the Silurian record. Journal of the Geological Society (London) 147, 663–674.

Jin, J., Copper, P., 2004. Species-level response of tropical brachiopods to environmental crisis during the Late Ordovician mass extinction event. In: Best, M., Caron, J.-B. (Ed.), Canadian Paleontology Proceedings vol. 2, pp. 31–32.

Kaljo, D., Hints, L., Martma, T., Nõlvak, J., Oraspõld, A., 2004. Late Ordovician carbon isotope trend in Estonia, its significance in stratigraphy and environmental analysis. Palaeogeography, Palaeoclimatology, Palaeoecology 210, 165–185.

Koren', T.N., Oradovskaya, M.M., Pylma, L.J., Sobolevskaya, R.F., Chugaeva, M.N., 1983. The Ordovician and Silurian boundary in the north-east of the USSR. Trudy Mezhvedomstvennogo Stratigraficheskogo Komiteta SSSR vol. 11. Nauka, Leningrad. (in Russian).

Kump, L.R., Arthur, M.A., 1999. Interpreting carbon-isotope excursions: carbonates and organic matter. Chemical Geology 161, 181–198.

Kump, L.R., Arthur, M.A., Patzkowski, M.E., Gibbs, M.T., Pinkus, D.S., Sheehan, P.M., 1999. A weathering hypothesis for glaciation at high atmospheric p_{CO_2} during the Late Ordovician. Palaeogeography, Palaeoclimatology, Palaeoecology 152, 173–187.

Long, D.G.F., 1993a. Oxygen and carbon isotopes and event stratigraphy near the Ordovician–Silurian boundary, Anticosti Island Quebec. Palaeogeography, Palaeoclimatology, Palaeoecology 104, 49–59.

Long, D.G.F., 1993b. Limits on Late Ordovician eustatic sea-level change from carbonate shelf sequences: an example from Anticosti Island, Quebec. International Association of Sedimentologists Special Paper 18, 487–499.

Long, D.G.F., Copper, P., 1987. Late Ordovician sand-wave complexes on Anticosti Island Quebec: a marine tidal embayment. Canadian Journal of Earth Sciences 24, 1821–1832.

McCrea, J.M., 1950. On the isotopic chemistry of carbonates and a paleotemperature scale. Journal of Chemical Physics 18 (6), 849–857.

Melchin, M.J., 1989. Llandovery graptolite biostratigraphy and paleobiogeography, Cape Phillips Formation, Canadian Arctic Islands. Canadian Journal of Earth Sciences 26, 1726–1746.

Melchin, M.J., 2002. Restudy of some Ordovician–Silurian boundary graptolites from Anticosti Island: implications for the age and correlation of the Ellis Bay Formation. Canadian Paleontology Conference, Program and Abstracts No. 12, Ottawa, September, 2002, pp. 31–33.

Melchin, M.J., Mitchell, C.E., 1991. Late Ordovician extinction in the Graptoloidea. In: Barnes, C.R., Williams, S.H. (Eds.), Advances in Ordovician Geology, Paper-Geological Survey of Canada vol. 90-9, pp. 143–156.

Melchin, M.J., McCracken, A.D., Oliff, F.J., 1991. The Ordovician–Silurian boundary on Cornwallis and Truro islands Arctic Canada: preliminary data. Canadian Journal of Earth Sciences 28, 1854–1862.

Melchin, M.J., Holmden, C., Williams, S.H., 2003. Correlation of graptolite biozones, chitinozoan biozones, and carbon isotope curves through the Hirnantian. In: Albanesi, G.L., Beresi, M.S., Peralta, S.H. (Eds.), Ordovician from the Andes, INSUEGO, Serie de Correlación Geológica vol. 17, pp. 101–104.

Munnecke, A., Samtleben, C., Bickert, T., 2003. The Ireviken Event in the lower Silurian of Gotland, Sweden relation to similar Palaeozoic and Proterozoic events. Palaeogeography, Palaeoclimatology, Palaeoecology 195, 99–124.

Murphy, J.B., Fernández-Suárez, J., Jeffries, T.E., 2004. Lithogeochemical and Sm–Nd and U–Pb isotope data from the Silurian–Lower Devonian Arisaig Group clastic rocks, Avalon terrane, Nova Scotia: a record of terrane accretion in the Appalachian–Caledonide orogen. Geological Society of America Bulletin 116, 1183–1201.

Nõlvak, J., 1999. Ordovician chitinozoan biozonation of Baltoscandia. Acta Universitatis Carolinae–Geologica 43 (1/2), 287–290.

Owen, A.W., Robertson, D.B.R., 1995. Ecological changes during the end-Ordovician extinction. Modern Geology 20, 21–39.

Panchuk, K.M., Holmden, C., Kump, L.R., in press-a. Sensitivity of the epeiric sea C-isotope record to local-scale C-cycle processes: tales from the Mohawkian Sea. Palaeogeography, Palaeoclimatology, Palaeoecology.

Panchuk, K.M., Holmden, C., Leslie, S.A., in press-b. Local controls on carbon cycling in the Ordovician Midcontinent region of North America with implications for carbon isotope secular curves. Journal of Sedimentary Research.

Pancost, R.D., Freeman, K.H., Patzkowsky, M.E., 1999. Organic-matter source variation and the expression of a late Middle Ordovician carbon isotope excursion. Geology 27, 1015–1018.

Patterson, W.P., Walter, L.M., 1994. Depletion of ^{13}C in seawater ΣCO_2 on modern carbonate platforms: significance for the carbon isotopic record of carbonates. Geology 2, 885–888.

Riva, J., 1988. Graptolites at and below the Ordovician–Silurian boundary on Anticosti Island, Canada. Bulletin of the British Museum, Natural History. Geology 43, 221–237.

Sheehan, P.M., 2001. The Late Ordovician mass extinction. Annual Review of Earth and Planetary Sciences 29, 331–364.

Soufiane, A., Achab, A., 2000. Chitinozoan zonation of the Late Ordovician and the Early Silurian of the island of Anticosti, Quebec, Canada. Review of Palaeobotany and Palynology 109, 85–111.

Underwood, C.J., Crowley, S.F., Marshall, J.D., Brenchley, P.J., 1997. High-resolution carbon isotope stratigraphy of the basal Silurian stratotype (Dob's Linn, Scotland) and its global correlation. Journal of the Geological Society (London) 154, 709–718.

Van Staal, C., Dewey, J.F., MacNiocaill, C., McKerrow, W.S., 1998. The Cambrian–Silurian tectonic evolution of the northern Appalachians and British Caledonides: history of a complex, west and southwest Pacific-type segment of Iapetus. In: Blundell, D.J., Scott, A.C. (Eds.), Lyell: The Past is the Key to the Present, Special Publication-Geological Society of London vol. 143, pp. 199–242.

Verniers, J., Vandenbroucke, T., Nielsen, 2005. Chitinozoan biozonation at the Ordovician–Silurian transition in Dob's Lin (Scotland, U.K.) and Lönstorp (Scania, Sweden). The Dynamic Silurian Earth. In: Eriksson, M.E., Calner, M. (Eds.), Field Meeting of the Subcommision on Silurian Stratigraphy 2005, Gotland, Rapporter och meddelanden-Sveriges Geologiska Undersökning vol. 121, pp. 96–97.

Wang, K., Chatterton, B.D.E., Wang, Y., 1997. An organic carbon isotope record of Late Ordovician to Early Silurian marine sedimentary rocks Yangtze, Sea South China: implications for CO_2 changes during the Hirnantian glaciation. Palaeogeography, Palaeoclimatology, Palaeoecology 132, 147–158.

Williams, S.H., 1983. The Ordovician–Silurian boundary graptolite fauna of Dob's Linn, southern Scotland. Palaeontology 26 (3), 605–639.

Zalasiewicz, J., Tunnicliff, S., 1994. Uppermost Ordovician to Lower Silurian graptolite biostratigraphy of the Wye Valley, central Wales. Palaeontology 37, 695–720.